This article has been accepted for publication in a future issue of this journal, but has not been fully edited. Content may change prior to final publication. Citation information: DOI 10.1109/TMECH.2017.2674701, IEEE/ASME Transactions on Mechatronics



# MPC for Robot Manipulators with Integral Sliding Modes Generation

Gian Paolo Incremona, *Member, IEEE*, Antonella Ferrara, *Senior Member, IEEE*, and Lalo Magni

***Abstract*—This paper deals with the design of a robust hierarchical multi-loop control scheme to solve motion control problems for robot manipulators. The key elements of the proposed control approach are the inverse dynamics-based feedback linearized robotic MIMO system and the combination of a Model Predictive Control (MPC) module with an Integral Sliding Mode (ISM) controller. The ISM internal control loop has the role to compensate the matched uncertainties due to unmodelled dynamics, which are not rejected by the inverse dynamics approach. The external loop is closed relying on the MPC, which guarantees an optimal evolution of the controlled system while fulfilling state and input constraints. The motivation for using ISM, apart from its property of providing robustness to the scheme with respect to a wide class of uncertainties, is also given by its capability of enforcing sliding modes of the controlled system since the initial time instant, allowing one to solve the model predictive control optimization problem relying on a set of linearized decoupled SISO systems which are not affected by uncertain terms. The proposal has been verified and validated in simulation, relying on a model of a COMAU Smart3-S2 industrial robot manipulator, identified on the basis of real data.**

***Index Terms*—Model predictive control, integral sliding mode, robot manipulators, uncertain systems.**

## I. Introduction

IN robotics technology recent research trends focus on performing particularly critical tasks in an optimal way, while fulfilling some plant constraints in order to avoid failures, wear of the electromechanical parts or to guarantee safe and close robot-human interactions [1], [2]. Yet, typically, industrial robots are controlled by classical PD or PID controllers [2], which can fail in guaranteeing this kind of features.

In the last decades, among the control algorithms published in the literature, Model Predictive Control (MPC) represents an appropriate and effective solution to solve this kind of problem, providing an optimal control strategy in case of even complex constrained dynamical systems [3]–[6]. Hence, the online optimization typically can lead to an increased computation time with respect to “classical” control laws. For this reason, MPC has been efficiently used in several industrial processes, such as chemical plants or oil refineries [7], but its application to robotic systems in a true industrial environment, in which unavoidable modelling uncertainties and external disturbances affect the system, is still limited [8]–[11].

Moreover, the MPC method requires the knowledge of the dynamical model of the system, according to which the optimal control sequence is generated by predicting the future evolution of the state variables. Since possible modelling uncertainties can occur, recent research has been devoted to develop robust MPC approaches able to satisfy the system constraints even in these critical cases [12], [13]. In this direction, the two main approaches proposed in the literature are the so-called min-max approach, able to fulfill the plant constraints considering the worst possible uncertainty realization, but at the price of a very high computational burden [14]–[16], and the so-called open-loop nominal approach, where the real constraints are shrunk to guarantee that the original constraints are fulfilled for any possible uncertainty realization [17]–[19].

G. P. Incremona and A. Ferrara are with the Dipartimento di Ingegneria Industriale e dell'Informazione, University of Pavia, Via Ferrata 5, 27100 Pavia, Italy (e-mail: gp.incremona@gmail.com, antonella.ferrara@unipv.it).

L. Magni is with the Dipartimento di Ingegneria Civile e Architettura, University of Pavia, Via Ferrata 3, 27100 Pavia, Italy (e-mail: lalo.magni@unipv.it).

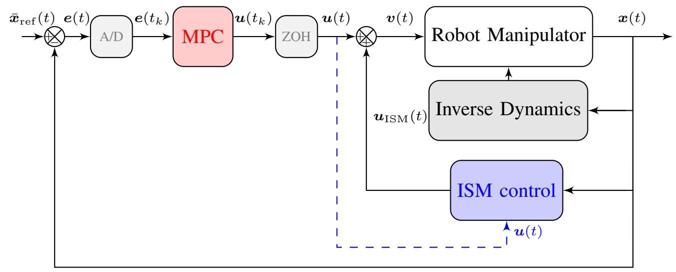


Figure 1. Scheme of the overall hierarchical multi-loop control scheme for robot manipulators

In this paper, inspired by [20], taking into account the class of robot manipulators, and having the aim of keeping the computational complexity to a minimum, in order to make the proposal really usable in practice, an alternative robust hierarchical multi-loop control scheme is proposed (see Figure 1). More specifically, the control scheme consists of three loops: an inner loop based on the so-called Inverse Dynamics approach [2], aimed at transforming the nonlinear MIMO robotic system into a set of perturbed linearized decoupled SISO systems (the number of systems is equal to the number of the joints of the robot manipulator); a second loop including a controller designed according to the so-called Integral Sliding Mode (ISM) control approach [21], which has the role of rejecting at a higher rate all the matched uncertainties [22], [23]; finally, an external loop involving a controller of MPC type with the role of guaranteeing the optimal evolution of the controlled system in the respect of state and input constraints. By the virtue of the linearizing and decoupling effects of the Inverse Dynamics approach, and of the capability of the ISM controller to make the controlled system insensitive to matched uncertainties since the initial time instant, standard linear MPC methodology [5], running at a slower rate, can be designed in the outer loop, with a clear benefit in terms of containment of computational complexity. A preliminary version of this work without proofs of the generalized approach and evaluation of the computational costs has been presented in [24].

This article has been accepted for publication in a future issue of this journal, but has not been fully edited. Content may change prior to final publication. Citation information: DOI 10.1109/TMECH.2017.2674701, IEEE/ASME Transactions on Mechatronics



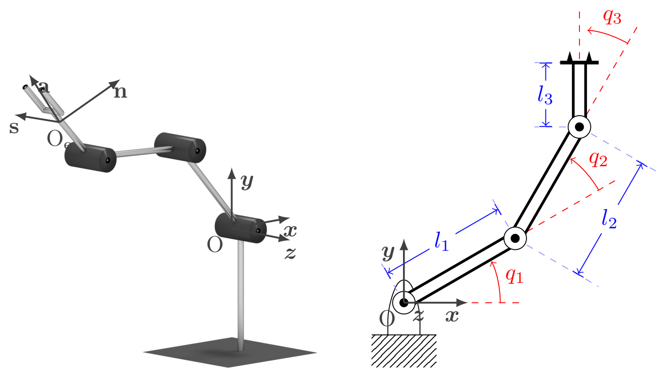


(a) spatial view (b) planar view

Figure 2. Anthropomorphic robot manipulator with three joints. **(a)** spatial schematic view with base-frame and end-effector frame. **(b)** planar schematic view with joints and links numeration

The present paper is organized as follows. In Section II, the model of the robotic system is introduced, and dynamical aspects are recalled. In Section III, the Inverse Dynamics approach is described and the control problem to solve is formulated. In Section IV, the proposed control scheme is discussed, illustrating the ISM control component and the MPC control law, while in Section V the stability analysis is reported. Section VI is devoted to present simulation results obtained by relying on the model of an industrial manipulator, i.e., a COMAU Smart3-S2 anthropomorphic robot. Both the model and the noise used in simulation have been identified on the basis of experimental tests, so that the simulation environment is quite realistic. Finally, keeping in mind an implementation in practical cases, the computational cost of the proposed algorithm is also discussed.

## II. The Robot Model

In order to formulate the model of a generic $n$-joints robot system, dynamical aspects have to be recalled.

For the sake of simplicity, without lost of generality, refer to the three joints ($n=3$) robot manipulator schematically shown in Figure 2b. Let $l_i$, $i=1,2,\ldots n$ denote the length of the $i$-th link, $q_1$ denote the orientation of the first link with respect to $\boldsymbol{x}$-axis clockwise positive, and $q_j$, $j=2,3,\ldots n$, denote the displacement of the $j$-th link with respect to the $(j-1)$-th one clockwise positive. Let $O-\{\boldsymbol{x},\boldsymbol{y},\boldsymbol{z}\}$, denote the base-frame of the robotic manipulator, and $O_{\mathrm{e}}-\{\mathbf{n},\mathbf{s},\mathbf{a}\}$ denote the end-effector frame as indicated in Figure 2a.

The dynamics of the robot can be written in the joint space, by using the Lagrangian approach, as

$$\boldsymbol{M}(\boldsymbol{q})\ddot{\boldsymbol{q}}+\boldsymbol{n}(\boldsymbol{q},\dot{\boldsymbol{q}})=\boldsymbol{\tau} \quad (1)$$

$$\boldsymbol{n}(\boldsymbol{q},\dot{\boldsymbol{q}})=\boldsymbol{C}(\boldsymbol{q},\dot{\boldsymbol{q}})\dot{\boldsymbol{q}}+\boldsymbol{F}_{\mathrm{v}}\dot{\boldsymbol{q}}+\boldsymbol{F}_{\mathrm{s}}\,\mathrm{sgn}(\dot{\boldsymbol{q}})+\boldsymbol{g}(\boldsymbol{q}) \quad (2)$$

where $\boldsymbol{M}(\boldsymbol{q})\in\mathbb{R}^{n\times n}$ is the inertia matrix, $\boldsymbol{C}(\boldsymbol{q},\dot{\boldsymbol{q}})\in\mathbb{R}^{n\times n}$ represents centripetal and Coriolis torques, $\boldsymbol{F}_{\mathrm{v}}\in\mathbb{R}^{n\times n}$ is the viscous friction matrix, $\boldsymbol{F}_{\mathrm{s}}\in\mathbb{R}^{n\times n}$ is the static friction matrix, $\boldsymbol{g}(\boldsymbol{q})\in\mathbb{R}^{n}$ is the vector of gravitational torques and $\boldsymbol{\tau}\in\mathbb{R}^{n}$ represents the motors torques.

## III. Problem Formulation

In this section, the considered globally feedback linearized MIMO system will be introduced and the corresponding state-space model will be defined.

### A. Inverse Dynamics Control

In order to reduce the nonlinear MIMO robotic system to a linear system, the so-called *Inverse Dynamics* approach [2] is used. The inverse dynamics of the robot manipulator can be written, in the joint space, as a nonlinear relationship between the plant inputs and the plant outputs, relying on (1)-(2), so that the control law can be expressed as

$$\boldsymbol{\tau}=\boldsymbol{M}(\boldsymbol{q})\boldsymbol{v}+\hat{\boldsymbol{n}}(\boldsymbol{q},\dot{\boldsymbol{q}}) \quad (3)$$

where $\boldsymbol{v}$ is an auxiliary control variable. Typically, the identified $\boldsymbol{M}(\boldsymbol{q})$ coincides with the actual one, while $\hat{\boldsymbol{n}}$ is an estimate of $\boldsymbol{n}$, which does not necessarily coincide with $\boldsymbol{n}$ [25]. By applying the feedback linearization to system (1)-(2), the resulting model is

$$\ddot{\boldsymbol{q}}=\boldsymbol{v}-\boldsymbol{\eta}(\boldsymbol{q},\dot{\boldsymbol{q}}) \quad (4)$$

where $\boldsymbol{\eta}(\boldsymbol{q},\dot{\boldsymbol{q}})$ takes into account the modelling uncertainties and external disturbances, i.e.,

$$\boldsymbol{\eta}(\boldsymbol{q},\dot{\boldsymbol{q}})=-\boldsymbol{M}^{-1}(\boldsymbol{q})(\hat{\boldsymbol{n}}(\boldsymbol{q},\dot{\boldsymbol{q}})-\boldsymbol{n}(\boldsymbol{q},\dot{\boldsymbol{q}}))\,. \quad (5)$$

### B. State-Space Model

After the application of the Inverse Dynamics control, the original MIMO system is reduced to $n$ SISO decoupled systems, one for each joint, in which the state vector is $\boldsymbol{x}_i=[x_{1_i}\,x_{2_i}]^T=[q_i\,\dot{q}_i]^T$, while $\eta_i$ represents the so-called matched uncertainty [22] such that

$$\begin{cases}\dot{x}_{1_i}(t)=x_{2_i}(t)\\ \dot{x}_{2_i}(t)=v_i(t)-\eta_i(t)\end{cases} \quad (6)$$

which is a double integrator, with $\dot{x}_{2_i}=\ddot{q}_i$ being the acceleration of the $i$-th joint.

System (6) can be written in a matrix compact form as the following constrained linear SISO system

$$\dot{\boldsymbol{x}}_i(t)=\boldsymbol{A}_i\boldsymbol{x}_i(t)+\boldsymbol{B}_i(v_i(t)-\eta_i(t)) \quad (7)$$

where $\boldsymbol{x}_i\in\mathbb{R}^2$ is the state vector, $v_i\in\mathcal{U}$ is the current control variable, with $\mathcal{U}\subset\mathbb{R}$ being a compact set containing the origin point, and $\eta_i\in\mathbb{R}$ the disturbance term of the system. Moreover, $\boldsymbol{A}_i\in\mathbb{R}^{2\times 2}$, and $\boldsymbol{B}_i\in\mathbb{R}^{2\times 1}$ is full rank. Assume also that the state variables are restricted to fulfill the following constraint

$$\boldsymbol{x}_i\in\mathcal{X} \quad (8)$$

where $\mathcal{X}$ is a compact set containing the origin as an interior point, while the control variable is such that

$$\|v_i\|\leq v_{i_{\max}} \quad (9)$$

with $v_{i_{\max}}=\mathcal{U}^{\sup}:=\sup_{\boldsymbol{v}\in\mathcal{U}}\{\|\boldsymbol{v}\|\}$ being the limits of the actuators in terms of acceleration. The uncertainty term $\eta_i$ is also bounded such that

$$\eta_i\in\mathcal{D} \quad (10)$$

This article has been accepted for publication in a future issue of this journal, but has not been fully edited. Content may change prior to final publication. Citation information: DOI 10.1109/TMECH.2017.2674701, IEEE/ASME Transactions on Mechatronics



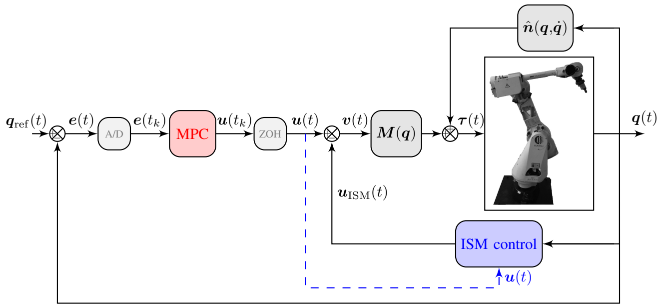


Figure 3. Detailed MPC/ISM control scheme applied to the considered feedback linearized robot manipulator COMAU Smart3-S2

where $\mathcal{D}$ is a compact set containing the origin with known $\mathcal{D}^{\sup} := \sup_{\boldsymbol{\eta}\in\mathcal{D}}\{\|\boldsymbol{\eta}\|\}$.

### C. Problem Statement

We are now in a position to be able to formulate the control problem to solve. Given the robot system described in Section II, the control objective is to design a control system in order to make the robot manipulator track a pre-specified reference trajectory. In the following section, a functional multi-rate architecture which combines a MPC module and an ISM controller is designed to solve the aforementioned control problem. The role of the MPC is to make the robot manipulator follow the reference trajectories in an optimal way with respect to input and output constraints. The ISM control rejects matched disturbances and uncertain terms due to unmodelled dynamics, which are not compensated by the Inverse Dynamics approach.

## IV. Model Predictive Control/Integral Sliding Mode Control: The Control Strategy

Making reference to the general control scheme in Figure 1, the control law is designed on the basis of the feedback linearized system (7). More specifically, the whole auxiliary control variable $\boldsymbol{v}(t)$ is chosen as follows

$$\boldsymbol{v}(t) = \boldsymbol{u}(t) + \boldsymbol{u}_{\mathrm{ISM}}(t) \tag{11}$$

where $\boldsymbol{u}$ and $\boldsymbol{u}_{\mathrm{ISM}}$ are generated by the MPC controller and the ISM controller, respectively. The ISM controller is based on the continuous-time model of the system and on the signal generated by the MPC controller, which, in turn, is based on the discrete-time model of the original system. For the sake of simplicity, in the following subsections we consider only the single SISO system and the subscript $i$ is omitted, when it is obvious.

### A. The Considered Control Scheme

In Figure 3 the proposed control scheme is illustrated in detail. This scheme consists of three control loops. The first loop is based on the Inverse Dynamics approach, described in Section III. After the inverse dynamics feedback linearization, the second loop is closed relying on the ISM controller which computes $\boldsymbol{u}_{\mathrm{ISM}} \in \mathbb{R}^n$ and rejects the matched uncertainty affecting the system. The third loop is designed to implement the MPC based controller which computes the control $\boldsymbol{u} \in \mathbb{R}^n$ combined with $\boldsymbol{u}_{\mathrm{ISM}}$ so as to solve the reference tracking problem in an optimal way while satisfying the constraints. The position error of the controlled system, given as input to the MPC module, is defined as $\boldsymbol{e} = \boldsymbol{q}_{\mathrm{ref}} - \boldsymbol{q}$, $\boldsymbol{q}_{\mathrm{ref}}$ being the desired reference trajectory.

### B. Integral Sliding Mode Controller

The ISM control has the feature to provide robustness to the scheme in front of a wide class of uncertainties, and to enforce sliding modes of the controlled system since the initial time instant. This control approach requires i) the knowledge of a *nominal model* of a system that can be also nonlinear, ii) a properly designed high level control law (MPC in our case), and iii) a discontinuous control action in order to remove the uncertain terms. Considering the dynamic system (6), assume that, for each joint, the so-called integral sliding variable $\sigma_i \in \mathbb{R}$ (see [21]) is defined as follows

$$\sigma_i(\boldsymbol{x}_i(t)) = \boldsymbol{S}_i\left(\boldsymbol{x}_i(t) - \boldsymbol{x}_i(t_0) - \int_{t_0}^{t}[x_{2_i}(\zeta),\, u_i(\zeta)]^T d\zeta\right) \tag{12}$$

with $\sigma_i(x_i(t)) = 0$ being the associated integral sliding manifold, $t_0$ the initial time instant, $\boldsymbol{S}_i$ the row vector $[c_i,\, 1]$, and $c_i$ a positive constant.

Now, the control law can be expressed as follows

$$u_{i_{\mathrm{ISM}}} = -U_{i_{\max}}\,\mathrm{sgn}(\sigma_i) \tag{13}$$

where $U_{i_{\max}} > \mathcal{D}^{\sup}$ is suitably chosen in order to enforce the sliding mode, with $\mathcal{D}^{\sup}$ depending on the modelling uncertainties and disturbances (5).

*Remark 1:* Note that ISM control can imply the so-called chattering phenomenon [26] which can be avoided by using integral higher order sliding modes as that in [27]. □

Having in mind a robotic application, as shown in [21], an effective solution, able to cope with chattering and avoid high frequency switching of the variable structure component of the control torque, consists in using the so-called *equivalent control* [22]. The equivalent control cannot be computed, since it depends on the uncertain terms affecting the system. However, in [21], it is shown that an approximation of the equivalent control can be obtained via a first order linear filter with the real discontinuous control (13) as input signal, i.e.,

$$\tilde{u}_{i_{\mathrm{ISM_{eq}}}}(t) = \frac{1}{\mu_i}\int_{t_0}^{t} \mathrm{e}^{-\frac{1}{\mu_i}(t-\zeta)} u_{i_{\mathrm{ISM}}}(\zeta)d\zeta \tag{14}$$

where $\mu_i$ is the time constant of the filter, while the sliding variable has to be redesigned as

$$\sigma_i(\boldsymbol{x}_i(t)) = \boldsymbol{S}_i\left(\boldsymbol{x}_i(t) - \boldsymbol{x}_i(t_0) - \int_{t_0}^{t}[x_{2_i}(\zeta),\, v_i(\zeta) - u_{i_{\mathrm{ISM}}}(\zeta)]^T d\zeta\right) \tag{15}$$

with $v_i(t) = u_i(t) + \tilde{u}_{i_{\mathrm{ISM_{eq}}}}(t)$. Note that, since a first order linear filter is used to obtain the equivalent control, the sliding variable has to be modified as in (15) so to take into account the difference between the filtered control (14)

This article has been accepted for publication in a future issue of this journal, but has not been fully edited. Content may change prior to final publication. Citation information: DOI 10.1109/TMECH.2017.2674701, IEEE/ASME Transactions on Mechatronics



and the discontinuous one (13), intrinsically compensating the mismatch between the actual equivalent control, $u_{i_{\text{ISM}_{\text{eq}}}}$, and its average value, $\tilde{u}_{i_{\text{ISM}_{\text{eq}}}}$. This implies that the sliding manifold is continuously adapted in order to guarantee the ideal sliding mode generation $\forall\, t \geq t_0$.

The effect of the ISM control law is that of rejecting the uncertainty of system (6) so as to obtain

$$\begin{cases} \dot{x}_{1_i}(t) = x_{2_i}(t) \\ \dot{x}_{2_i}(t) = u_i(t) \end{cases} \tag{16}$$

that is

$$\dot{\boldsymbol{x}}_i(t) = \boldsymbol{A}_i \boldsymbol{x}_i(t) + \boldsymbol{B}_i u_i(t) \tag{17}$$

which is a double integrator without disturbances affecting the system. Note that the ISM control cannot violate the state constraints due to the fact that the sliding variable also depends on the MPC control law.

*Remark 2:* As suggested in [21], the time constant $\mu_i$ should be set such that the fundamental component of the discontinuous action is not distorted. □

### C. Model Predictive Controller

By virtue of the rejection of matched uncertainties and external disturbances through the use of the ISM controller, the MPC controller can be designed starting from the nominal system, i.e., the dynamical system without matched uncertainties. For this reason it is not necessary to consider conservative robust MPC approaches [16], [19], but only a nominal MPC is required, with a significant beneficial effect in terms of computational burden. In the following, for the sake of simplicity, the subscript $i$ will be omitted, when obvious.

The MPC controller is designed on the discrete time system of (17), i.e.,

$$\boldsymbol{x}_i(t_{k+1}) = \widetilde{\boldsymbol{A}}_i \boldsymbol{x}_i(t_k) + \widetilde{\boldsymbol{B}}_i u_i(t_k)\ . \tag{18}$$

Note that, for the design of a continuous time MPC and a rigorous proof of stability, one can refer to [28]. The adopted MPC controller is based on the solution of the so-called Finite-Horizon Optimal Control Problem (FHOCP). The latter consists in minimizing, at any sampling time $t_k$, a suitably defined cost function with respect to the control sequence $\mathbf{u}_{[t_k, t_{k+N-1}|t_k]} := [u_0(t_k), u_1(t_k), \ldots, u_{N-1}(t_k)]$, where $N \geq 1$ is the prediction horizon. In our case, the cost function to minimize with respect to $\mathbf{u}_{[t_k, t_{k+N-1}|t_k]}$ is a quadratic function as

$$J(\boldsymbol{e}_i(t_k), \mathbf{u}_{i_{[t_k, t_{k+N-1}|t_k]}}, N) = \sum_{j=0}^{N-1} \|\boldsymbol{e}_i(t_{k+j})\|^2_{\boldsymbol{Q}_i} + \|u_i(t_{k+j})\|^2_{R_i} + \|\boldsymbol{e}_i(t_{k+N})\|^2_{\boldsymbol{\Pi}_i} \tag{19}$$

where the notation $\|\cdot\|^2_{\boldsymbol{W}}$ stands for the square norm of a vector weighted by a matrix $\boldsymbol{W}$.

The cost function (19) is subject to the hard constraints represented by the dynamics of system (18), and inequalities constraints on states and input variables, i.e.,

$$\boldsymbol{x}_i(t_{k+j}) \in \mathcal{X} \tag{20}$$

$$\boldsymbol{x}_i(t_{k+N}) \in \mathcal{X}_{\text{f}} \tag{21}$$

$$\|u_i(t_{k+j})\| \leq v_{i_{\max}} - U_{i_{\max}} \tag{22}$$

with $j = 1, \ldots, N-1$. Moreover, $\mathcal{X}_{\text{f}}$ is the so-called terminal set such that $\boldsymbol{x}_i(t_{k+N}) \in \mathcal{X}_{\text{f}}$, with

$$\mathcal{X}_{\text{f}} := \{\boldsymbol{x}_i \mid \|\boldsymbol{x} - \bar{\boldsymbol{x}}_{i_{\text{ref}}}\|^2_{\boldsymbol{\Pi}} \leq \rho\}, \quad \mathcal{X}_{\text{f}} \subseteq \mathcal{X} \tag{23}$$

for any constant $\bar{\boldsymbol{x}}_{i_{\text{ref}}} \in \mathcal{X}_{\text{ref}}$ such that $(\bar{\boldsymbol{x}}_{i_{\text{ref}}}, 0)$ is an equilibrium point for systems (18) and with $\mathcal{X}_{\text{f}}$ containing the origin as an interior point. In order to define the terminal set and the terminal penalty, one needs to introduce an auxiliary control law $\kappa_{i_{\text{f}}}(\boldsymbol{e}_i)$ that can be

$$\kappa_{i_{\text{f}}}(\boldsymbol{e}_i(t_k)) = \boldsymbol{K}_{\text{LQ}} \boldsymbol{e}_i(t_k) \tag{24}$$

$\boldsymbol{K}_{\text{LQ}}$ being the control gain of an infinite horizon Linear-Quadratic (LQ) controller with the same cost function. Note that, the value $\rho$ in (23) is a positive real number such that $\forall\, \boldsymbol{x}_i(t_{\bar{k}}) \in \mathcal{X}_{\text{f}}$, $\forall\, t_k > t_{\bar{k}}$ it yields,

$$\boldsymbol{x}_i(t_k) \in \mathcal{X}_{\text{f}} \tag{25}$$

$$\|\kappa_{i_{\text{f}}}(\boldsymbol{e}_i(t_k))\| \leq v_{i_{\max}} - U_{i_{\max}} \tag{26}$$

with $\boldsymbol{e}_i(t_k) = \boldsymbol{x}_i(t_k) - \bar{\boldsymbol{x}}_{i_{\text{ref}}}(t_k)$. In (19), $\boldsymbol{Q}_i$ is a positive definite matrix, $R_i$ is a scalar weight, and $\boldsymbol{\Pi}_i$ is the positive definite terminal state weight associated with the terminal penalty $V_{\text{f}} = \|\boldsymbol{e}_i(t_{k+N})\|^2_{\boldsymbol{\Pi}_i}$ which is assumed such that

$$V_{\text{f}}(\boldsymbol{e}_i(t_{k+1})) - V_{\text{f}}(\boldsymbol{e}_i(t_k)) + \|\boldsymbol{e}_i(t_k)\|^2_{\boldsymbol{Q}_i} + \|\kappa_{i_{\text{f}}}(\boldsymbol{e}_i(t_k))\|^2_{R_i} \leq 0 \tag{27}$$

so as to ensure the stability of the controlled system. The matrix $\boldsymbol{\Pi}_i$ represents instead the solution of the *Riccati equation*,

$$(\widetilde{\boldsymbol{A}}_i - \widetilde{\boldsymbol{B}}_i \boldsymbol{K}_{\text{LQ}})^T \boldsymbol{\Pi}_i (\widetilde{\boldsymbol{A}}_i - \widetilde{\boldsymbol{B}}_i \boldsymbol{K}_{\text{LQ}}) - \boldsymbol{\Pi}_i = -\boldsymbol{Q}_i - \boldsymbol{K}^T_{\text{LQ}} R_i \boldsymbol{K}_{\text{LQ}}. \tag{28}$$

Then, according to the Receding Horizon strategy, the applied piecewise-constant control law is the following

$$u_i(t) = \kappa_{\text{MPC}}(\boldsymbol{e}_i(t_k)),\ t \in [t_k,\, t_{k+1}) \tag{29}$$

where $t_{k+1} - t_k = T$ is the MPC sampling time, and

$$\kappa_{\text{MPC}}(\boldsymbol{e}_i(t_k)) := u^{\text{o}}_{i_0}(t_k) \tag{30}$$

with $u^{\text{o}}_{i_0}(t_k)$ the first value at $t_k$ of the optimal control sequence for the $i$-th joint, obtained by solving the FHOCP.

## V. Stability Analysis

With reference to the proposed control approach, the following results can be proved.

*Lemma 1:* Given the MIMO nonlinear robotic model (1) and (2), by applying the Inverse Dynamics approach in (3), one obtains $n$ decoupled perturbed double integrators. □

*Proof:* The proof of this lemma in case of an ideal compensation is reported in [2]. Since unavoidable modelling uncertainties are present, applying the Inverse Dynamics (3) to (1), one obtains

$$\ddot{\boldsymbol{q}} = \boldsymbol{v} + \boldsymbol{M}^{-1}(\boldsymbol{q})(\hat{\boldsymbol{n}}(\boldsymbol{q}, \dot{\boldsymbol{q}}) - \boldsymbol{n}(\boldsymbol{q}, \dot{\boldsymbol{q}})) = \boldsymbol{v} - \boldsymbol{\eta}(\boldsymbol{q}, \dot{\boldsymbol{q}}) \tag{31}$$

This article has been accepted for publication in a future issue of this journal, but has not been fully edited. Content may change prior to final publication. Citation information: DOI 10.1109/TMECH.2017.2674701, IEEE/ASME Transactions on Mechatronics



with the uncertain terms such that (5) holds. Hence, the result is a set of $n$ decoupled perturbed double integrators as

$$\begin{cases} \dot{x}_{1_i}(t) = x_{2_i}(t) \\ \dot{x}_{2_i}(t) = v_i(t) - \eta_i(t) \end{cases} \tag{32}$$

with $x_{1_i} = q_i$ and $x_{2_i} = \dot{q}_i$, $i = 1, \ldots, n$, which concludes the proof. ■

*Lemma 2:* Given system (7), controlled via (11), (14) and (29), with the sliding variable (15) such that the matrix $\boldsymbol{S}_i\boldsymbol{B}_i$ is nonsingular, then an integral sliding mode is enforced on the integral sliding manifold $\sigma_i = 0$, $\forall\, t \geq t_0$. □

*Proof:* The proof directly follows from [21] (see also [29, Chapter 7] for further details), according to which the fact that an integral sliding mode is enforced since the initial time instant $t_0$ can be straight forward using the Lyapunov Second Method by considering the function $V_{\mathrm{ISM}_i} = 0.5\sigma_i^2$ as Lyapunov candidate. ■

In the following theorem, the equivalent system controlled by the MPC component will be obtained and the role of the ISM component as *perturbation estimator* will be exploited.

*Theorem 1:* Given system (7), controlled via (11), (14) and (29), then $\forall\, t \geq t_0$ the equivalent system results in being

$$\dot{\boldsymbol{x}}_i(t) = \boldsymbol{A}_i\boldsymbol{x}_i(t) + \boldsymbol{B}_i u_i(t)$$

with $i = 1, \ldots, n$. □

*Proof:* By virtue of Lemma 1 and Lemma 2, since the initial time instant $t_0$ one has that $\sigma_i = 0$ so that also its time derivative is $\dot{\sigma}_i = 0$, i.e.,

$$\begin{aligned} \dot{\sigma}_i &= \boldsymbol{S}_i\dot{\boldsymbol{x}}_i - \boldsymbol{S}_i[x_{2_i}\ u_i + \tilde{u}_{i_{\mathrm{ISM_{eq}}}} - u_{i_{\mathrm{ISM}}}]^T \\ &= c_i x_{2_i} + v_i - \eta_i - c_i x_{2_i} - u_i - \tilde{u}_{i_{\mathrm{ISM_{eq}}}} + u_{i_{\mathrm{ISM}}} \\ &= u_i + \tilde{u}_{i_{\mathrm{ISM_{eq}}}} - \eta_i - u_i - \tilde{u}_{i_{\mathrm{ISM_{eq}}}} + u_{i_{\mathrm{ISM}}} = 0\,. \end{aligned} \tag{33}$$

According to the *equivalent control* concept (see [22] for a definition), one has that in Filippov sense

$$0 = u_i + \tilde{u}_{i_{\mathrm{ISM_{eq}}}} - \eta_i - u_i - \tilde{u}_{i_{\mathrm{ISM_{eq}}}} + u_{i_{\mathrm{ISM_{eq}}}} = u_{i_{\mathrm{ISM_{eq}}}} - \eta_i\,.$$

Hence, one can conclude that $u_{i_{\mathrm{ISM_{eq}}}} = \eta_i$. Substituting the latter expression into system (7), controlled via (11), the equivalent system results in being (17), which proves the theorem. ■

Starting from Lemma 1, Lemma 2 and Theorem 1, the following theorem can be proved.

*Theorem 2:* Given system (18), controlled via (29), obtained by solving the FHOCP with cost function (19) subject to the system dynamics, input and state constraints (20)-(21), then, $\boldsymbol{x}_i = \bar{\boldsymbol{x}}_{i_{\mathrm{ref}}}$, $\forall\, i = 1, \ldots, n$, results in being an asymptotically stable equilibrium point of the controlled system. □

*Proof:* The proof of the theorem has to be carried out in two steps. First, it is necessary to prove the recursive feasibility, i.e., given an optimal solution at time $t_k$, it is always possible to find a solution at time $t_{k+1}$ that satisfies all the constraints.

*Step 1 (Feasibility)* Consider the optimal solution given at $t_k$, $\mathbf{u}^{\circ}_{i_{[t_k, t_{k+N-1}|t_k]}} := [u^{\circ}_{i_0}(t_k), u^{\circ}_{i_1}(t_k), \ldots, u^{\circ}_{i_{N-1}}(t_k)]$. According to the Receding Horizon principle, only the first element of the optimal sequence is applied. At the time instant $t_{k+1}$ the control sequence

$$\widetilde{\mathbf{u}}_{i_{[t_{k+1}, t_{k+N}|t_{k+1}]}} = \begin{cases} \mathbf{u}^{\circ}_{i_{[t_{k+1}, t_{k+N-1}|t_k]}} \\ \kappa_{i_{\mathrm{f}}}(\boldsymbol{e}_i(t_{k+N})) \end{cases} \tag{34}$$

fulfills the constraints (20), (21), and (22). In fact, since it holds $\widetilde{\mathbf{u}}_{i_{[t_{k+1}, t_{k+N-1}|t_{k+1}]}} = \mathbf{u}^{\circ}_{i_{[t_{k+1}, t_{k+N-1}|t_k]}}$, constraints (20) and (22) are fulfilled. Moreover, from (21), it holds that $\boldsymbol{x}_i(t_{k+N}) \in \mathcal{X}_{\mathrm{f}}$. Hence, from (26), it also holds that $\|\kappa_{i_{\mathrm{f}}}(\boldsymbol{e}_i(t_{k+N}))\| \leq v_{i_{\max}} - U_{i_{\max}}$ and $\boldsymbol{x}_i(t_{k+N}) \in \mathcal{X}$, so that (20) and (22) are satisfied also for $j = N$. Finally, from (25), it follows that $\boldsymbol{x}_i(t_{k+N+1}) \in \mathcal{X}_{\mathrm{f}}$, which concludes the proof of the feasibility.

After having proved the recursive feasibility, the second step is to prove the stability properties of the system controlled via the MPC law.

*Step 2 (Stability)* In order to prove the asymptotical stability, we need to find a Lyapunov function candidate. We chose the function $J^{\circ}(\boldsymbol{e}_i(t_k), t_k) > 0, \forall\ \boldsymbol{e}_i \neq \boldsymbol{0}$, and $J^{\circ}(\boldsymbol{0}, t_k) = 0$, associated with the cost function (19). Consider the cost function $\widetilde{J}(\boldsymbol{e}_i(t_{k+1}), t_{k+1})$ associated with the feasible control sequence (34). Since, this function is not a priori the optimal one, it holds $J^{\circ}(\boldsymbol{e}_i(t_{k+1}), t_{k+1}) \leq \widetilde{J}(\boldsymbol{e}_i(t_{k+1}), t_{k+1})$. From (19), by using (27), one has that

$$\begin{aligned} &\widetilde{J}(\boldsymbol{e}_i(t_{k+1}), t_{k+1}) - J^{\circ}(\boldsymbol{e}_i(t_k), t_k) \\ &= -\|\boldsymbol{e}_i(t_k)\|^2_{\boldsymbol{Q}_i} - \|\kappa_{i_{\mathrm{f}}}(\boldsymbol{e}_i(t_k))\|^2_{R_i} + V_{\mathrm{f}}(\boldsymbol{e}_i(t_{k+N+1})) + \\ &-V_{\mathrm{f}}(\boldsymbol{e}_i(t_{k+N})) + \|\boldsymbol{e}_i(t_{k+N})\|^2_{\boldsymbol{Q}_i} + \|\kappa_{i_{\mathrm{f}}}(\boldsymbol{e}_i(t_{k+N}))\|^2_{R_i} \\ &< -\|\boldsymbol{e}_i(t_k)\|^2_{\boldsymbol{Q}_i} - \|\kappa_{i_{\mathrm{f}}}(\boldsymbol{e}_i(t_k))\|^2_{R_i} < 0 \end{aligned} \tag{35}$$

which implies that $J^{\circ}$ is a decreasing function. Then, one can conclude that $\boldsymbol{x}_i = \bar{\boldsymbol{x}}_{i_{\mathrm{ref}}}$, $\forall\, i = 1, \ldots, n$, results in being an asymptotically stable equilibrium point of the controlled system, which concludes the proof. ■

## VI. A Case Study

The robotic system we are dealing with is a 6-joint robot manipulator. For the sake of simplicity, we consider only vertical planar motions of the robotic manipulator, locking three of the six joints of the robot. However, the proposed control scheme and the design of the controllers could have a more general validity, even in the spatial case for 6-joint robot manipulators.

The control strategy, previously proposed, has been applied in simulation to the model of a COMAU Smart3-S2 anthropomorphic industrial robot by using the software MATLAB Simulink. Note that the model has been identified on the basis of real data through experimental tests [25], so that the simulation environment is quite realistic.

The simulation scenario has also been made more realistic by injecting the disturbance terms $\boldsymbol{\eta} = [\eta_1, \eta_2, \eta_3]^T$ to the acceleration of the joints on the basis of the effective disturbances registered during experimental tests [27]. These disturbances represent modelling uncertainties, such as friction, centripetal or Coriolis forces, which are not completely compensated by the Inverse Dynamics control (3). The corresponding bounds of the uncertainties for joints 1, 2, 3 are $20,\ 30,\ 80\,\mathrm{rad\,s^{-2}}$, respectively. Moreover, according to the

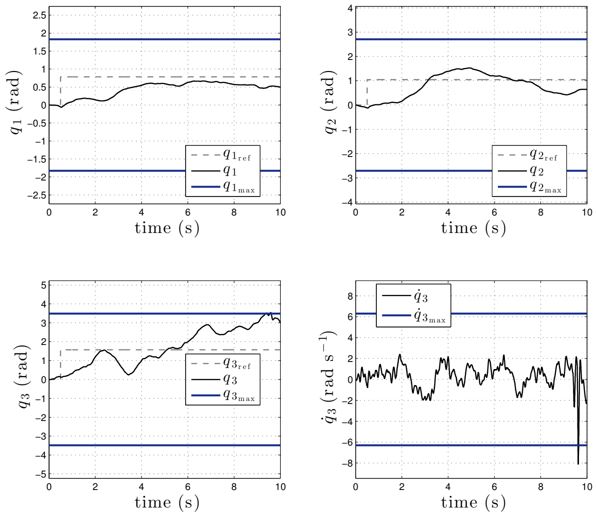


Figure 4. Time evolution of the joint variables for each joint, and the velocity $\dot{q}_3$ when only the nominal MPC is used

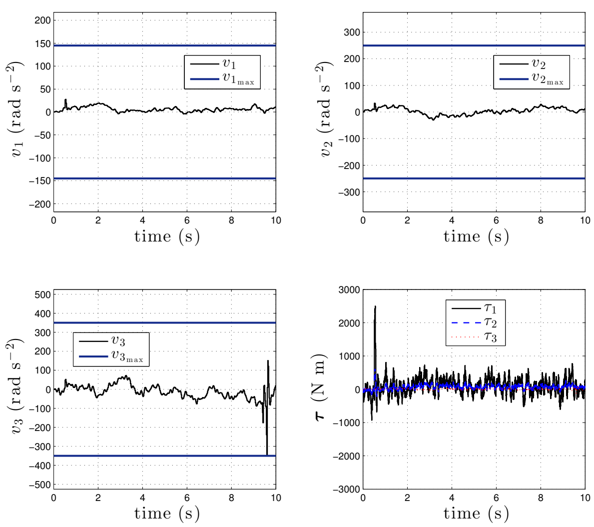


Figure 5. Time evolution of the auxiliary control variables and of the torque for each joint when only the nominal MPC is used

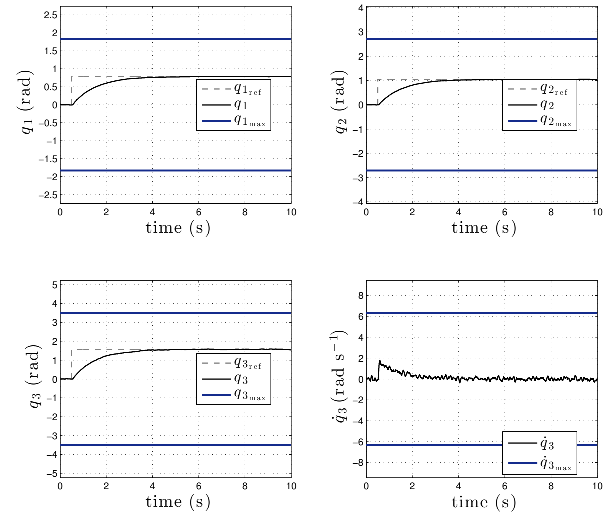


Figure 6. Time evolution of the joint variables for each joint, and the velocity $\dot{q}_3$ when the MPC/ISM strategy is used

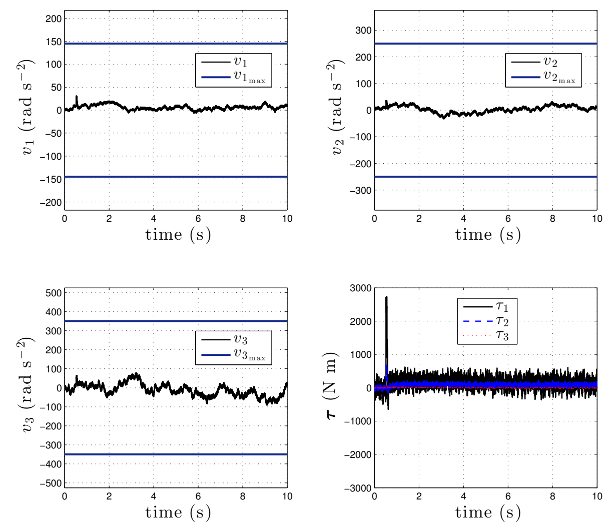


Figure 7. Time evolution of the auxiliary control variables and of the torque for each joint when the MPC/ISM strategy is used

Table I
STATE AND INPUT CONSTRAINTS FOR EACH JOINT

| Joint $i$ | $q_{i_{\max}}$ (rad) | $\dot{q}_{i_{\max}}$ (rad s$^{-1}$) | $v_{i_{\max}}$ (rad s$^{-2}$) |
|---|---|---|---|
| 1 | 1.83 | 2 | 145 |
| 2 | 2.71 | 3.5 | 250 |
| 3 | 3.49 | 6.3 | 350 |

mechanical limits of the real robot, the position, velocity and acceleration constraints are those reported in Table I. Note that, these values are the same provided by the robot manufacturer and imposed by the limit switches fastened on the real system. The initial conditions of the joint variables are $\boldsymbol{q}_0 = [0,\ 0,\ 0]^T$, while the target position is $\boldsymbol{q}_{\mathrm{ref}} = [\pi/4,\ \pi/3,\ 2\pi/4]^T$. In order to show the effectiveness of the control law (11), the latter is compared with the case in which a nominal MPC without ISM control is applied to the robot manipulator. The sliding variable has been chosen as in (15) with $c_i = 10$, $i = 1,\ 2,\ 3$, the ISM control is as in (14), while the ISM control gains are 20, 35 and 85, respectively. The MPC parameters have been chosen such that for each joint $\boldsymbol{Q}_i = \mathrm{diag}(100,\ 100)$, $R_i = 0.1$, and the terminal weight equal to

$$\boldsymbol{\Pi}_i = \begin{bmatrix} 5213.4 & 165.8 \\ 165.8 & 221.3 \end{bmatrix} . \qquad (36)$$

Moreover, the sampling time of the simulation has been set as in the real case equal to $t_{\mathrm{s}} = 0.001\,\mathrm{s}$, while the sampling time of the MPC loop has been set as $T = 0.02\,\mathrm{s}$, with prediction horizon $N = 10$.

### *A. Results and Comparison*

The tracking control performance is evaluated through the following indexes: the root mean square (RMS) error ($e_{\mathrm{RMS}}$)

This article has been accepted for publication in a future issue of this journal, but has not been fully edited. Content may change prior to final publication. Citation information: DOI 10.1109/TMECH.2017.2674701, IEEE/ASME Transactions on Mechatronics



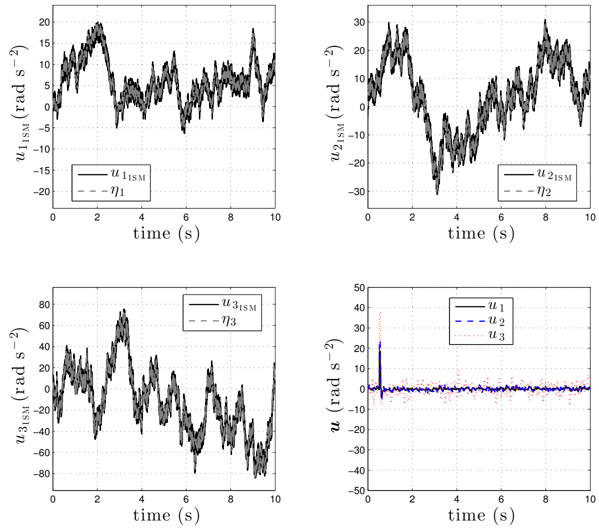


Figure 8. Time evolution of the ISM control component with respect to the matched uncertainty affecting the system, and the MPC component when the MPC/ISM strategy is used

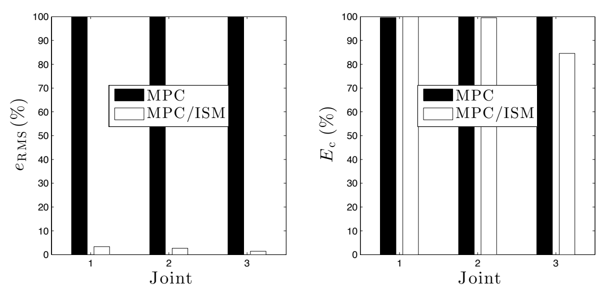


Figure 9. Performance indexes normalized with respect to the worse case

Table II
PERFORMANCE INDEXES FOR EACH JOINT

| Strategy | Joint $i$ | $e_{\mathrm{RMS}_i}$ (rad) | $E_{\mathrm{c}_i}$ (rad s$^{-2}$) |
|---|---|---|---|
| MPC | 1 | 0.2105 | 8.0303 |
| | 2 | 0.3749 | 13.4839 |
| | 3 | 1.0458 | 41.2172 |
| MPC/ISM | 1 | 0.0070 | 8.0600 |
| | 2 | 0.0102 | 13.4217 |
| | 3 | 0.0152 | 34.8530 |

Table III
TIME CONSUMPTION OF THE PROPOSED CONTROL STRATEGY IN SECONDS

| Algo. | mean | min. | max. | std. dev. |
|---|---|---|---|---|
| MPC | 0.018 | 0.017 | 0.71 | 0.011 |
| ISM | $2.9 \times 10^{-5}$ | $2.7 \times 10^{-5}$ | 0.0086 | $1.4 \times 10^{-4}$ |

and the RMS value of the control action ($E_{\mathrm{c}}$). Table II shows the outcome indexes achieved through the MPC standalone and the proposed MPC/ISM strategy. The RMS error in steady-state is significantly smaller when the MPC/ISM is used for all the joints with respect to the case with only MPC. This is clearly represented in Figure 4 where the uncertainty strongly affects the position tracking performance and the state constraints are violated (see position and velocity of joint 3), when only MPC is used. Figure 5 shows the corresponding auxiliary control variables and the torques directly fed into the plant. On the other hand, a very precise tracking with constraints satisfaction can be observed in Figure 6 when the MPC/ISM control is applied. The corresponding auxiliary control variables and torques are illustrated in Figure 7. This beneficial effect is given by the ISM component which perfectly estimates and rejects the uncertain terms affecting the systems (Figure 8). As for the control effort, it results in being very similar in both cases, except for Joint 3 for which it is smaller in case of MPC/ISM control, as can be observed in the graphical rendering of the performance indexes, normalized with respect to the worse cases, in Figure 9.

### B. *Evaluation of Application*

To evaluate the computational costs of the proposed control strategy in practical robotic cases, an implementation in MATLAB code, with *quadprog* as MPC solver, running on a laptop-computer with an Intel Core 2 Duo at 2.4 GHz with 4 GB RAM, has been performed. The time measurement has been made over four thousand executions of each algorithm. This can be considered as a conservative upperbound of a practical implementation made with any imperative assembly language. Table III reports the results expressed in terms of mean, minimum, maximum and standard deviation of the execution time. Their respective sum for each algorithm is an estimation of the total execution time. As expected the higher computational burden is required by the MPC component, but by virtue of the reduction of the complexity of the optimization problem relying on a simple constrained linear system, it results in being reasonable to be implemented in any standard recent robot control unit or embedded systems such as FPGA (Field Programmable Gate Array). As for the ISM component, the obtained execution time confirms its computational lightweight which makes ISM control a powerful easy-to-implement solution even in an industrial field.

## VII. CONCLUSIONS

In this paper a hierarchical multi-loop control scheme based on the combination of Model Predictive Control and Integral Sliding Mode control has been proposed to solve motion control problems for robot manipulators. A basic Inverse Dynamics feedback linearizing approach is applied to obtain a set of linearized decoupled SISO systems. The Integral Sliding Mode control, which runs at higher rate, makes the systems insensitive to the matched uncertainties presence. Finally, the external loop is characterized by the Model Predictive Control component with the aim to ensure the optimal evolution of the controlled system in the respect of state and input constraints, while keeping the computational complexity to a minimum. This makes the proposal really usable in practice, as also verified by evaluating the possible computational costs of the involved algorithms. The proposed control scheme has been

This article has been accepted for publication in a future issue of this journal, but has not been fully edited. Content may change prior to final publication. Citation information: DOI 10.1109/TMECH.2017.2674701, IEEE/ASME Transactions on Mechatronics



validated in simulation relying on a realistic model of an industrial COMAU Smart3-S2 robot manipulator, identified on the basis of experimental tests.

## REFERENCES


[1] B. Siciliano and O. Khatib, Eds., *The Handbook of Robotics*. Springer, 2008.

[2] B. Siciliano, L. Sciavicco, L. Villani, and G. Oriolo, *Robotics-Modelling, Planning and Control*, 3rd ed. Springer-Verlag, 2009, pp. 248–302.

[3] M. Morari and J. H. Lee, "Model predictive control: past, present and future," *Computers & Chemical Engineering*, vol. 23, no. 4, pp. 667–682, May 1999.

[4] D. Q. Mayne, J. B. Rawlings, C. V. Rao, and P. O. M. Scokaert, "Constrained model predictive control: Stability and optimality," *Automatica*, vol. 36, no. 6, pp. 789 – 814, Jun. 2000.

[5] J. B. Rawlings and D. Q. Mayne, *Model Predictive Control: Theory and Design*. Nob Hill Pub, Llc, 2009.

[6] D. Q. Mayne, "Model predictive control: recent developments and future promise," *Automatica*, vol. 50, no. 12, pp. 2967–2986, Dec. 2014.

[7] S. Qin and T. Badgwell, "A survey of industrial model predictive control technology," *Control Engineering Practice*, vol. 11, no. 7, pp. 733–764, Jul. 2003.

[8] V. Duchaine, S. Bouchard, and C. M. Gosselin, "Computationally efficient predictive robot control," *IEEE/ASME Transactions on Mechatronics*, vol. 12, no. 5, pp. 570–578, Oct. 2007.

[9] J. C. L. Barreto S., A. G. S. Conceição, C. E. T. Dórea, L. Martinez, and E. R. de Pieri, "Design and implementation of model-predictive control with friction compensation on an omnidirectional mobile robot," *IEEE/ASME Transactions on Mechatronics*, vol. 19, no. 2, pp. 467–476, Apr. 2014.

[10] J. Yang, W. X. Zheng, S. Li, B. Wu, and M. Cheng, "Design of a prediction-accuracy-enhanced continuous-time MPC for disturbed systems via a disturbance observer," *IEEE Transactions on Industrial Electronics*, vol. 62, no. 9, pp. 5807–5816, Sep. 2015.

[11] E. Kayacan, H. Ramon, and W. Saeys, "Robust trajectory tracking error model-based predictive control for unmanned ground vehicles," *IEEE/ASME Transactions on Mechatronics*, vol. 21, no. 2, pp. 806–814, Apr. 2016.

[12] L. Magni, G. De Nicolao, R. Scattolini, and F. Allgower, "Robust model predictive control for nonlinear discrete-time systems," *International Journal of Robust and Nonlinear Control*, vol. 13, no. 3–4, pp. 229–246, Feb. 2003.

[13] L. Magni, D. M. Raimondo, and F. Allgöwer, *Nonlinear Model Predictive Control: Towards New Challenging Applications*, ser. Lecture Notes in Control and Information Sciences. Springer Science & Business Media, 2009.

[14] P. O. M. Scokaert and D. Q. Mayne, "Min-max feedback model predictive control for constrained linear systems," *IEEE Transactions on Automatic Control*, vol. 43, no. 8, pp. 1136–1142, Aug. 1998.

[15] A. Bemporad, F. Borrelli, and M. Morari, "Min-max control of constrained uncertain discrete-time linear systems," *IEEE Transactions on Automatic Control*, vol. 48, no. 9, pp. 1600–1606, Sep. 2003.

[16] F. A. C. C. Fontes and L. Magni, "Min-max model predictive control of nonlinear systems using discontinuous feedbacks," *IEEE Transactions on Automatic Control*, vol. 48, no. 10, pp. 1750–1755, Oct. 2003.

[17] L. Chisci, J. A. Rossiter, and G. Zappa, "Systems with persistent disturbances: predictive control with restricted constraints," *Automatica*, vol. 37, no. 7, pp. 1019–1028, Jul. 2001.

[18] G. Grimm, M. J. Messina, S. E. Tuna, and A. R. Teel, "Nominally robust model predictive control with state constraints," *IEEE Transactions on Automatic Control*, vol. 52, no. 10, pp. 1856–1870, Oct. 2007.

[19] D. Limon Marruedo, T. Alamo, F. Salas, and E. F. Camacho, "Input to state stability of min-max MPC controllers for nonlinear systems with bounded uncertainties," *Automatica*, vol. 42, no. 5, pp. 797–803, May 2006.

[20] M. Rubagotti, D. M. Raimondo, A. Ferrara, and L. Magni, "Robust model predictive control with integral sliding mode in continuous-time sampled-data nonlinear systems," *IEEE Transactions on Automatic Control*, vol. 56, no. 3, pp. 556–570, Mar. 2011.

[21] V. I. Utkin and J. Shi, "Integral sliding mode in systems operating under uncertainty conditions," in *Proc. 35th IEEE Conference on Decision and Control*, vol. 4, Kobe, Japan, Dec. 1996, pp. 4591–4596.

[22] V. Utkin, *Sliding Modes in Control and Optimization*, ser. Communication and control engineering. Springer-Verlag, 1992.

[23] C. Edwards and S. Spurgeon, *Sliding Mode Control: Theory and Applications*, ser. Systems and Control. Taylor & Francis, 1998.

[24] A. Ferrara, G. P. Incremona, and L. Magni, "A robust MPC/ISM hierarchical multi-loop control scheme for robot manipulators," in *Proc. 52th IEEE Conference on Decision and Control*, Florence, Italy, Dec. 2013, pp. 3560–3565.

[25] A. Calanca, L. M. Capisani, A. Ferrara, and L. Magnani, "Mimo closed loop identification of an industrial robot," *IEEE Transactions on Control Systems Technology*, vol. 19, no. 5, pp. 1214–1224, Sep. 2011.

[26] A. Levant, "Chattering analysis," *IEEE Transactions on Automatic Control*, vol. 55, no. 6, pp. 1380–1389, Jun. 2010.

[27] A. Ferrara and G. P. Incremona, "Design of an integral suboptimal second order sliding mode controller for the robust motion control of robot manipulators," *IEEE Transactions on Control Systems Technology*, vol. 23, no. 6, pp. 2316–2325, May 2015.

[28] L. Magni and R. Scattolini, "Model predictive control of continuous-time nonlinear systems with piecewise constant control," *IEEE Transactions on Automatic Control*, vol. 49, no. 6, pp. 900–906, Jun. 2004.

[29] V. I. Utkin, J. Guldner, and J. Shi, *Sliding Model Control in Electromechanical Systems*. Taylor and Francis, 1999.


**Gian Paolo Incremona** is a Post-Doc at Identification and Control of Dynamic Systems Laboratory of the University of Pavia. He was a student of the *Almo Collegio Borromeo* of Pavia, and of the class of *Science and Technology* of the Institute for Advanced Studies *IUSS* of Pavia. He received the Bachelor and Master degrees (with highest honor) in Electric Engineering, and the Ph.D. degree in Electronics, Electric and Computer Engineering from the University of Pavia, Italy, in 2010, 2012 and 2016, respectively. From October 2014 to December 2014, he was with the Dynamics and Control Group at the Eindhoven Technology University, Netherlands. His research interests include nonlinear control, variable structure control of sliding mode type, model predictive control, networked control, industrial robotics, power systems and glycemia control in diabetic subjects. He has been a member of the *IEEE* since September 2010.

**Antonella Ferrara** is Full Professor of Automatic Control at the University of Pavia. Her research deals with sliding mode and nonlinear control with application to traffic, automotive and robotics. She has authored/co-authored more than 300 papers, including more than 90 journal papers. She was *Associate Editor* of the *IEEE Transactions on Control Systems Technology* and of the *IEEE Transactions on Automatic Control*. Since January 2014, she is *Associate Editor* of the IEEE Control Systems Magazine. She is *Senior Member* of the *IEEE Control Systems Society*, and, among others, member of the *IEEE Technical Committee on Variable Structure and Sliding Mode Control*, and of the *IFAC Technical Committee on Transportation Systems*. Since July 2013 she is *Chair* of the *Women in Control Standing Committee of the Control Systems Society*.

**Lalo Magni** is Full Professor of Automatic Control at the University of Pavia. From October 1996 to February 1997 and in March 1998 he was at CESAME, Universitè Catholique de Louvain, Louvain La Neuve, Belgium. From October to November 1997 he was at the University of Twente with the System and Control Group in the Faculty of Applied Mathematics. He was plenary, semi-plenary or Keynote speaker at several international conferences. His current research interests include nonlinear control, predictive control, receding-horizon control, robust control, process control and artificial pancreas. His research is witnessed by more than 70 papers published in the main international journals. He served as an *Associate Editor* of the *IEEE Transactions on Automatic Control* and of *Automatica*. He was *Chair* of the *NMPC Workshop on Assessment and Future Direction*, September 2008, Pavia, Italy. He was the national principal investigator of a *FIRB project Futuro in Ricerca* and the local investigator of an *FP7 UE Program*.